Large suspension bridges to withstand wind loading

C. Borri, C. Costa, M. Majowiecki, L. Salvatori & P. Spinelli

CRIACIV (Centro Interuniversitario di Aerodinamica delle Costruzioni ed Ingegneria del Vento), Università di Firenze & IUAV Venezia, Italy

ABSTRACT:
Suspension bridges are the current technical solution to overcome long distances. In this paper, the traditional suspension scheme is compared with a different technical solution providing additional structural resources thanks to a system of cables with opposed curvature. Favorable effects of this scheme are evidenced, concerning wind resistance, regarding to serviceability conditions. Dynamic analyses in time domain are performed, within a FE framework capable to take into account structural nonlinearities and dynamic wind loads.

1 INTRODUCTION

Long-span bridges represent a great challenge in structural engineering. As a matter of fact, the current solution for very long-span bridges is the *suspension* scheme, as demonstrated by the recent achievements of Humber Bridge (UK, 1981, center span of 1410 m), Great Belt East Bridge (Denmark, 1998, 1624 m), Akashi-Kaikyo Bridge (Japan, 1998, 1991 m), and by the proposals for Messina Strait Crossing (Italy, 3300 m) and for Gibraltar Link (Gibraltar, 5000 m). Technical strategies are investigated in order to guarantee adequate resistance, structural resources against natural events, design economy.

In particular, suspension bridges evidence a strong sensitivity to the wind action. This problem has been mainly faced, since now, by acting on the *bridge deck* design, whether by increasing the torsional stiffness through a very rigid truss-girder (as preferred in Japan and U.S.), or by improving the aerodynamic performances through closed box or multi-box girders (mostly adopted in Europe).

These choices have been usually supported by intensive wind tunnel campaigns performed on cross-sectional models, in order to characterize the aerodynamic behavior of the selected deck.

Nevertheless, it is worth to point out that, for intrinsic scaling problems, it is not possible to reproduce in the wind channel the real flow. Moreover, the extension of cross-sectional results to the entire structure is not straightforward and free of uncertainties. Therefore, an extreme optimization based on such cross-sectional tests does not cover all the risks concerning the global behavior and it has no chance to capture significant three-dimensional phenomena, including turbulence effects, along-span vibrations, full-scale interaction between turbulence and self-excited loads (see Larsen et al., 2000).

It seems then troublesome to predict the behavior of the whole bridge in a safe and accurate manner.

On the other hand, a high level of reliability must be guaranteed for such a strategic structure. A strong optimization of the deck in the aerodynamic sense need to be supported by additional structural resources provided not only by the deck, but also by the global structural design.

In fact, an aerodynamic closed-box girder is unable to provide adequate torsional stiffness over a very long-span, while a truss girder would be inefficient for its weight and poor aerodynamics.

Therefore, a cooperating structural system composed by a deck supported by a multi-cable system could offer a convenient answer, as underlined by Astiz (1998).

This idea has been first suggested by S. Musmeci: an interesting structural model of suspension bridge integrated by means of stabilizing cables with opposed curvature has been proposed for the Messina bridge (Fig. 1). These secondary cables should provide additional stiffness and resistance not only against lift and torsional wind actions but also against drag, as they lie on a non-vertical plane. Such a structural redundancy results in additional safety, which could compensate some not-yet-experienced effects on super long spans. First static analyses on this topic have been carried out by Borri et al. (1993), evidencing smaller along-wind displacements.

In this paper, a detailed study on the efficiency of an analogous scheme is presented, under dynamic

loading, focusing the attention on the response to the wind action.

Two ideal schemes are considered and analysed by means of a suitable numerical code, capable of parametric generation of the structural model (Salvatori and Spinelli, 2005). Structural nonlinearities are included, as well as self-excited and buffeting loads.

First, drag effects are neglected and a simplified planar system is studied. A complete three-dimensional model will be considered as a further step.

Self-excited forces are described in time-domain by means of indicial functions, which have demonstrated their feasibility in the representation of complex aeroelastic phenomena (Costa, 2004).

Buffeting forces are traditionally modelled, according to Simiu and Scanlan (1996).

Tests are performed both in laminar and turbulent flow.

In order to show the advantages introduced by the proposed double-effect cable solution, its dynamical properties and its behaviour under wind excitation are compared with those of the classical scheme.

In particular, it is shown that the double-curvature solution presents some advantages in terms of serviceability conditions, while critical flutter velocity is strongly dependent on additional cable and deck mass and stiffness.

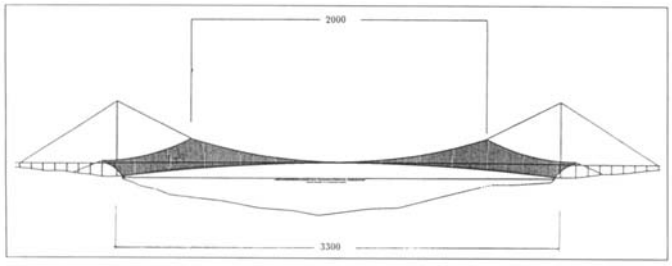

Figure 1. Musmeci's proposal for the Messina Strait Crossing.

2 MECHANICAL MODEL

A long suspension bridge consists, basically, of bridge towers, bridge deck, cables, suspenders, and anchorages.

A mechanical model having N degrees of freedom (DoFs) is examined. Equations of motion, for the linear case, can be written as follows

$$\mathbf{M}\ddot{\mathbf{q}}(t)+\mathbf{C}\dot{\mathbf{q}}(t)+\mathbf{K}\mathbf{q}(t)=\mathbf{F}(t) \qquad (1)$$

where the vector $\mathbf{q}$ of order N represents the displacement vector, $\mathbf{F}$ is the vector of external forces and $\mathbf{M}$, $\mathbf{C}$ and $\mathbf{K}$ are, respectively, inertia, damping and stiffness matrices.

2.1 *Suspension bridge ('Classical' solution)*

The classical scheme of suspension bridge provides two main cables connected to suspenders, hanging the bridge deck (Fig. 2 and Fig. 3).

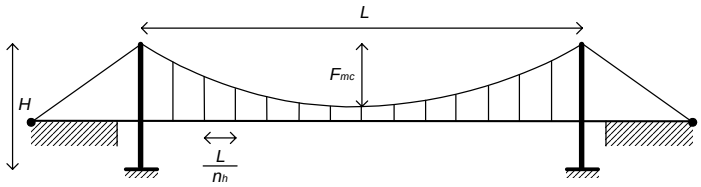

Figure 2. Reference structural model for classical suspension bridge.

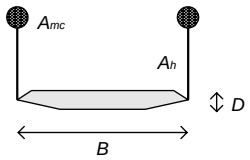

Figure 3. Reference cross-section for classical suspension bridge.

Geometry of the deck section is identified by the main characteristic dimensions, namely the *chord B*, and the *thickness D*. Pre-stress of the main cables (with area A_{mc}) is indicated with T_1. The area of hangers is referred to also as A_h.

2.2 *Suspension double-curvature bridge ('Musmeci' solution)*

A couple of cables with opposed curvature is added to the classical suspension scheme. Secondary cables are disposed in a vertical plane (Fig. 4 and Fig. 5).

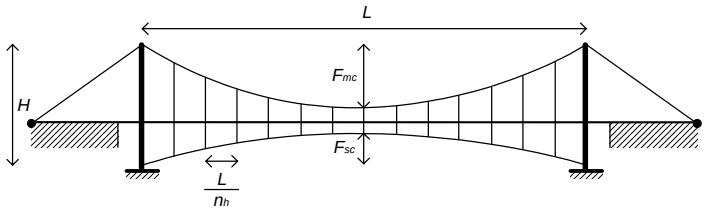

Figure 4. Reference structural model for '*Musmeci*' solution.

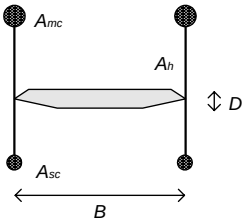

Figure 5. Reference cross-section for '*Musmeci*' solution.

A characteristic parameter of the structure is the pre-stress of the secondary cables, namely T_2. The area of secondary cables is A_{sc}.

3 WIND MODEL

Bridges are immersed in a turbulent wind field, assumed incompressible and non-viscous. Wind velocity U_{wind} is additively decomposed as a time-space variable field

$$\mathbf{U}_{wind}(M,t) = \mathbf{U}(M) + \mathbf{U}'(M,t) \tag{2}$$

where t is the time, $\mathbf{U}$ is the mean wind speed and $\mathbf{U}'$ represents a turbulent perturbation, acting at point M of coordinates $X(M)$, $Y(M)$ and $Z(M)$.

Mean wind is directed along the X axis, while the turbulence field has only one significant component, identified by w and directed along the vertical axis Z. The resultant wind field is then given by

$$\begin{aligned} U_{windX}(M,t) &= U(M) \\ U_{windY}(M,t) &= 0 \\ U_{windZ}(M,t) &= w(M,t) \end{aligned} \tag{3}$$

Assuming neutral conditions, the mean wind velocity U may be expressed by the logarithmic profile, while turbulence components are defined through an assigned power-spectral density and along-span coherence functions.

4 LOAD MODEL

Wind load, acting on each bridge deck section, is expressed as superposition of three components, namely a quasi-static (0), a buffeting (b) and a self-excited (se) action, directed along the global reference axes

$$\begin{aligned} F_X(t) &= F_{X0} + F_{Xb} + F_{Xse} \\ F_Z(t) &= F_{Z0} + F_{Zb} + F_{Zse} \\ M_Y(t) &= M_{Y0} + M_{Yb} + M_{Yse} \end{aligned} \tag{4}$$

4.1 *Quasi-static forces*

Static forces are due to dead loads and quasi-static wind action.

Quasi-static wind action is dependent only from the angle of attack α, that is from the relative placement of the bridge deck section with respect to the mean wind direction, through the aerodynamic coefficients $C_D(\alpha)$, $C_L(\alpha)$ and $C_M(\alpha)$. Such coefficients are usually measured in wind tunnel tests and are given with reference to the local sectional reference frame. In particular, subscripts D, L and M are referred, respectively, to drag force, lift force and aerodynamic moment, acting along the sectional chord, in the orthogonal direction and about the sectional center of mass.

Therefore, drag, lift and moment can be expressed as

$$\begin{aligned} F_D(t) &= qBC_D(\alpha) \\ F_L(t) &= qBC_L(\alpha) \\ M_a(t) &= qB^2C_M(\alpha) \end{aligned} \tag{5}$$

where $q = 1/2\rho U^2$ is the kinetic pressure and ρ is the air density.

Static forces identify the deflected position in which modal and linear time-domain dynamic analyses are performed.

4.2 *Buffeting forces*

Both quasi-steady and strip assumptions are accounted for in buffeting modeling. In particular, admittance functions take the values of unity and the action of turbulence on each section is assumed as independent from the action on the contiguous sections.

Buffeting forces are modeled, following the traditional quasi-steady formulation (Simiu and Scanlan 1996) and with reference to the wind field assigned in eqs. 3, as

$$\begin{aligned} F_{Db}(t) &= qBC_D \\ F_{Lb}(t) &= qB\left(\frac{dC_L}{d\alpha} + C_D\right)\frac{w}{U} \\ M_{ab}(t) &= qB^2\frac{dC_M}{d\alpha}\frac{w}{U} \end{aligned} \tag{6}$$

4.3 *Self-excited forces*

Self-excited forces are commonly modeled by means of frequency-dependent parameters (flutter derivatives) experimentally extracted and introduced in a time-domain framework. The original formulation is due to Scanlan and Tomko (1971), for a two-dimensional bridge deck section.

The complete thee-dimensional formulation, including terms related to drag force and horizontal motion, is proposed by Scanlan and Jones (1990) and recalled in eqs. (7), where P_i^*, H_i^* and A_i^* are the flutter derivatives (i = 1, …, 6).

Although such flutter derivatives offer the great advantage of being extracted through a consolidate experimental approach, they are is not well suited for time domain simulations, being expressed as function of reduced velocity $U_{red} = U/fB$ or reduced frequency $K = 2\pi/U_{red}$ where f is the response frequency.

$$
\begin{aligned}
F_{Dse}(t) &= qB\left\{KP_1^*\frac{\dot{p}}{U}+KP_2^*\frac{B\dot{\alpha}}{U}+K^2P_3^*\alpha+\right.\\
&\left.+K^2P_4^*\frac{p}{B}+KP_5^*\frac{\dot{y}}{U}+K^2P_6^*\frac{y}{B}\right\}\\
F_{Lse}(t) &= qB\left\{KH_1^*\frac{\dot{h}}{U}+KH_2^*\frac{B\dot{\alpha}}{U}+K^2H_3^*\alpha+\right.\\
&\left.+K^2H_4^*\frac{h}{B}+KH_5^*\frac{\dot{p}}{U}+K^2H_6^*\frac{p}{B}\right\}\\
M_{ase}(t) &= qB^2\left\{KA_1^*\frac{\dot{h}}{U}+KA_2^*\frac{B\dot{\alpha}}{U}+K^2A_3^*\alpha+\right.\\
&\left.+K^2A_4^*\frac{h}{B}+KA_5^*\frac{\dot{p}}{U}+K^2A_6^*\frac{p}{B}\right\}
\end{aligned}
\tag{7}
$$

An attractive alternative is offered by the pure time-domain formulation via indicial functions proposed by Scanlan et al. (1974) and further discussed by Borri & Höffer (2000) and Borri et al. (2002). The specific formulation of Costa (2004), arranged here for a three-dimensional structure, is adopted:

$$
\begin{aligned}
F_{Dse}(s) &= qB\frac{dC_D}{d\alpha}\left\{\Phi_{D\alpha}(0)\alpha(s)+\Phi_{Dy}(0)y'(s)+\right.\\
&+\Phi_{Dx}(0)x(s)+\int_0^s\Phi'_{D\alpha}(s-\tau)\alpha(\tau)d\tau+\\
&\left.+\int_0^s\Phi'_{D\alpha}(s-\tau)\alpha(\tau)d\tau+\int_0^s\Phi'_{D\alpha}(s-\tau)\alpha(\tau)d\tau\right\}\\
F_{Lse}(s) &= qB\frac{dC_L}{d\alpha}\left\{\Phi_{L\alpha}(0)\alpha(s)+\Phi_{Ly}(0)y'(s)+\right.\\
&+\Phi_{Lx}(0)x'(s)+\int_0^s\Phi'_{L\alpha}(s-\tau)\alpha(\tau)d\tau+\\
&\left.+\int_0^s\Phi'_{Ly}(s-\tau)y'(\tau)d\tau+\int_0^s\Phi'_{Lx}(s-\tau)x'(\tau)d\tau\right\}\\
M_{ase}(s) &= qB^2\frac{dC_M}{d\alpha}\left\{\Phi_{M\alpha}(0)\alpha(s)+\Phi_{My}(0)y'(s)+\right.\\
&+\Phi_{Mx}(0)x(s)+\int_0^s\Phi'_{M\alpha}(s-\tau)\alpha(\tau)d\tau+\\
&\left.+\int_0^s\Phi'_{My}(s-\tau)y'(\tau)d\tau+\int_0^s\Phi'_{Mx}(s-\tau)x'(\tau)d\tau\right\}
\end{aligned}
\tag{8}
$$

Self-excited forces are calculated via convolution integrals. Displacement histories are expressed as a series of infinitesimal step-wise increments. Non-stationary evolution in time of self-excited loads due to unit displacements is described by indicial functions. Three indicial functions are required for each force component. Each function is identified from the corresponding flutter derivatives.

This complete formulation, with respect to the other cited, include self-excited drag and horizontal motion. Analogous three–dimensional analyses can be performed by a modal approach (e.g. Chen and Kareem 2001, Scanlan and Jones, 1999), valuables only for linearized problems.

5 NUMERICAL MODELLING

The comprehensive program for the analysis of bridges under wind excitation developed by Salvatori and Spinelli (2005) has been adopted for the analyses. In fact, commercial programs can not consider history-dependent loads. The tool includes model generation, multi-correlated wind field generation, finite-element solver, as well as post-processing analyses, and allows an easier automatization of the simulations.

The pre-processing routine generates the FE model, given a few geometrical and mechanical characteristics (see Figs. 2-4). The number of modeled cross-section is an input for the pre-processor (here 10 sections have been used). The pre-processor also generates wind velocity time-histories of the through autoregressive (AR) algorithms.

As first step, a nonlinear static analysis under dead weight is performed. The modal analysis is then carried out in the statically deformed configuration, and the Rayleigh (linear) damping calculated. Finally, for each chosen value of the mean wind velocity, partially correlated wind time-histories are generated and time integrations (linear in this first study) are carried out.

6 STRUCTURAL ANALYSES

In this paper, the main goal is to emphasize the capabilities against wind action of the suspension double-curvature bridge, with respect to the classical suspension scheme.

Therefore, a first comparison is performed, between the two structural models, under different load conditions:

1. self-excited forces;
2. self-excited and buffeting forces.

In order to model properly self-excited forces, the identification of indicial functions is performed from aeroelastic derivatives, via a nonlinear least-square procedure.

First analyses are carried out for a mechanical model with a closed rectangular section characterized by dimensional ratio B/D = 12.5.

6.1 *Case study*

The case study pertains to the comparison between different technical schemes, characterized by equal

mechanical properties (Tab. 1): a '*Classical*' suspension and two '*Musmeci*' double-curvature bridges, characterized by different pre-stresses of the secondary cables, and indicated as *Musmeci*(1), and *Musmeci*(2).

Table 1. Mechanical properties common to the bridges (L=main span length; H=height of the towers; F=sag of the suspension cables; n_h=hanger number; J_x=equivalent flexural moment of inertia; J_x=equivalent torsional moment of inertia).

L [m]	B [m]	H [m]	m[kg/m]	A_{mc}[m^2]	J_x [m^4]
3300	52	378	$5.5\cdot10^4$	2.4153	8.418

D [m]	F_{mc} [m]	n_h [-]	I [kgm]	A_h [m^2]	J_y [m^4]
4.16	310	110	$2.8\cdot10^7$	0.0446	53.457

Additional properties required for the double-curvature suspension bridges '*Musmeci*' are the section of the secondary cables (A_{sc}=0.8189 m^2), the sag (F_{sc}=57 m) (see Fig. 4 and Fig. 5) and the pre-stress T_2: *Musmeci*(1) has a pre-stress of 37 kN/m, *Musmeci*(2) of 156 kN/m.

In the case with the lower pre-stress of 37 kN/m, analyses of double-curvature bridges are performed considering different materials for the stabilizing cables. In particular, Kevlar (*Musmeci*(1*k*)) and carbon fiber T300 (*Musmeci*(1*c*)) are taken into account. Main properties of such materials are collected in Tab .2.

Table 2. Main properties of materials used in double-curvature bridge (ρ=density; E=Young modulus).

Material	ρ[kN/m^3]	E [GPa]
Steel	78.00	170
Kevlar	14.50	131
Carbon Fiber T300	17.69	231

6.1.1 *Analyses with self-excited forces*

For the first study of a planar system, coefficients of indicial functions are taken from Costa (2004).
The first comparison between the two structural schemes concerns coupling frequencies and critical flutter condition. In particular, first six modes are shown in Tab. 3.a and Tab. 3.b. Vibration modes related to the carbon fiber model *Musmeci*(1*c*) are omitted, being practically identical to the modes of *Musmeci*(1*k*), indicating that the lightening of the masses produces the main benefits with respect to the change in the elastic modulus.

The accuracy of higher mode shapes depends on detailed modelling of the deck structure, which is not included in this study. The damping ratios are taken as 0.6%.

Critical flutter shape evidences, for all structures, the coupling of the two first vertical and torsional symmetric modes, as shown in details in Tab. 3.a and Tab. 3.b.

A lower critical flutter threshold, with respect to the classical model, can be observed in Tab. 4, because the frequencies of the vertical and torsional modes coupling at flutter become closer in the *Musmeci*'s structures. An increase of critical flutter speed is registered as the mass of the counter-opposed cables decreases, as in the *Musmeci*(1*k*) structure.

Table 3.a. Modal analyses of different structural solutions (V=vertical; T=torsional; S=symmetric; A=antisymmetric; *No*.=number of sines of the critical shape; *=modes coupling at flutter condition).

	Classical		*Musmeci(1)*	
	Period [s]	*Modal shape*	*Period* [s]	*Modal shape*
1	14.53	VA	13.20	VA
2	11.93	VS*	11.52	VS*
3	8.97	VS3	9.26	TS*
4	8.84	TS*	8.67	VS3
5	8.19	TA	8.23	TA
6	7.92	VA4	7.13	VA4

Table 3.b. Modal analyses of different structural solutions

	Musmeci(1k)		*Musmeci(2)*	
	Period [s]	*Modal shape*	*Period* [s]	*Modal shape*
1	13.18	VA	10.75	VA
2	11.20	VS*	10.53	VS*
3	8.81	TS*	8.93	TS*
4	8.50	VS3	7.47	TA
5	7.97	TA	7.27	VS3
6	7.11	VA4	5.69	VA4

Table 4. Flutter condition for different structural solutions.

	U_{cr} [m/s]	T_{cr} [s]	*Flutter Shape*
Classical	47	9.66	S
Musmeci(1)	38	9.87	S
Musmeci(1k)	40	9.45	S
Musmeci(2)	36	9.42	S

6.1.2 *Analyses with self-excited and buffeting forces*

Buffeting forces are simulated by adopting vertical wind autospectrum and cross-spectrum according to Simiu and Scanlan (1996) and considering the average elevation above the sea level of the bridge deck as 60m.

Main results concerns the maximum of the root mean square obtained for vertical (Fig. 6) and torsional displacement (Fig. 7). Even if a decreasing of the critical flutter velocity is observed, as the pre-stress of the secondary cables increases, a good behaviour is observed in serviceability conditions. In fact, displacements of the *Musmeci*'s solutions remain smaller than those of the '*Classical*' solution.

This is due also to the fact that energy content of turbulence is lower at high frequencies, and, therefore, vibration modes characterized by smaller pe-

riod, as the '*Musmeci*'s (Tab. 3.a and Tab. 3.b), result less excited by turbulent flow.

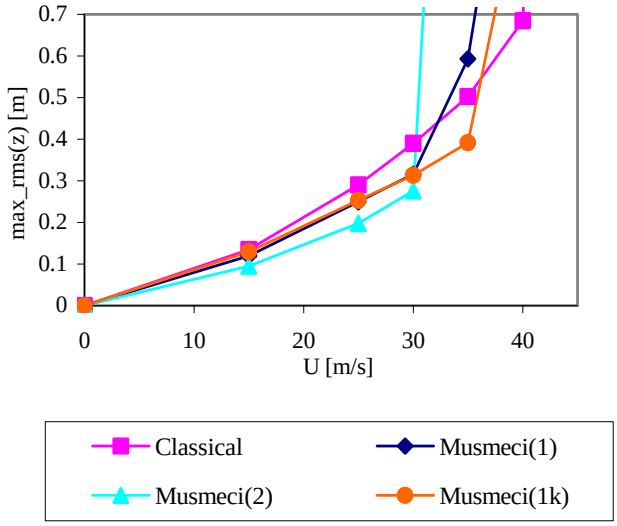

Figure 6. Maximum root-mean-square values of vertical displacement, for different structural schemes and various mean incoming velocities.

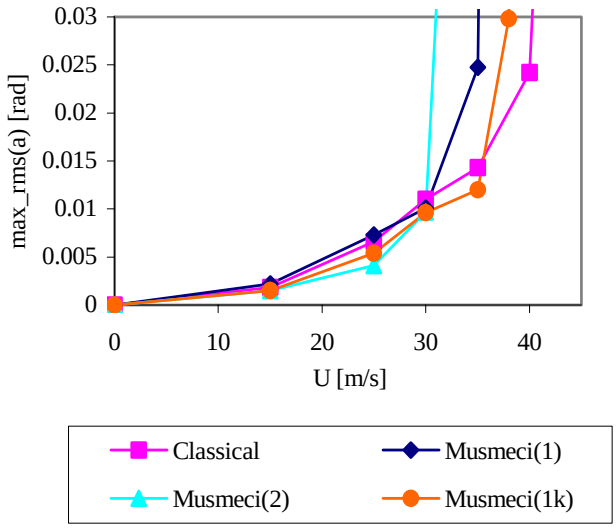

Figure 7. Maximum root-mean-square values of torsional displacement, for different structural schemes and various mean incoming velocities.

Moreover, the *Musmeci*(1*k*) solution presents a very good behaviour in serviceability conditions, guaranteeing the smallest displacements with the lowest pre-stress.

A significant trend can also be identified in Fig. 6 and Fig. 7, that is a more stiffened structure reaches the flutter threshold more 'rapidly', with respect to the '*Classical*' solution.

7 CONCLUSIONS

A comparison of the behaviour against the wind action of two structural schemes is presented. A '*Classical*' suspension scheme and two '*Musmeci*'-type solutions are accounted for, with stabilizing cables of different materials. Computer simulation techniques are used to generate wind forces on the bridge, including both buffeting and self-excited forces. Attention is focused on dynamic analyses, to evidence advantages and disadvantages of both schemes. In particular, it is shown that the '*Musmeci*' solutions present advantages in terms of serviceability conditions, under the action of turbulent flow. A strong dependence of critical flutter velocity on additional cable and deck mass and stiffness is, on the other hand, observed. Different combinations of geometries, mass and pre-stress can give rise to a wide scenario in terms of critical flutter velocity, being very important the modal shapes and frequency obtained. The double-curvature solution appears to be very interesting and further analyses are in progress. In particular, a even better efficiency is expected for non-planar cable systems and less 'engineered' deck aerodynamics.

ACKNOWLEDGEMENTS

The Authors gratefully acknowledge the financial support of the Cofinanced National Research Grant (COFIN) of the Ministry of University and Research (MIUR) 2001-2003.

REFERENCES

Astiz, M. A. 1998. Flutter stability of very long suspension bridges, *J. Bridge Eng*. 3-3, pp. 132-139.

Borri, C., Majowiecki, M. & Spinelli, P. 1993. The aerodynamic advantages of a double-effect large span suspension bridge under wind loading. *J. Wind Eng. Ind. Aerodyn.* Vol. 48, pp. 317-328.

Borri, C. & Hoffer, R. 2000. Aeroelastic wind forces on flexible girders. Meccanica, Vol. 35(10), pp. 1-15.

Chen, X., Matsumoto, M. & Kareem, A. 2000. Time domain flutter and buffeting response. Analysis of bridges. *J. Eng. Mech. ASCE*, Vol. 126(1), pp 7-16.

Costa, C.. 2004. Time-domain models in bridge deck aeroelasticity. Ph. D. Thesis, Università di Firenze, Italy

Katsuchi, H., Jones, N.P. & Scanlan, R.H. 1999. Multimode coupled flutter and buffeting analysis of the Akashi Kaikyo Bridge. *J. Struct. Eng., ASCE 125-1*: 60-70.

Larsen, A., Esdahl, S., Andersen, J. E. & Vejrum, T. 2000. Stœrebelt suspension bridge - vortex shedding excitation and mitigation by guide vanes. *J. Wind Eng. Ind. Aerodyn. 88*: 283-296.

Salvatori, L. & Spinelli, P. 2005. Effects of structural nonlinearities and along-span wind coherence on suspension bridge aerodynamics: some numerical simulation results. *Submitted*

Scanlan, R. H. & Tomko, A. 1971. Airfoil and Bridge Deck Flutter Derivatives, *J. Eng. Mech. Div*., vol. 97, ASCE, pp. 1717-1737.

Scanlan, R. H., Béliveau, J. & Budlong, K. S. 1974. Indicial aerodynamic functions for bridge decks. *J. Eng. Mech. Div*. 100-EM4, pp. 657-670.

Simiu, E. & Scanlan R. H. 1996. *Wind effects on Structures*. John Wiley & Sons, New York.